Merging-Beams Studies of Ba Collisions with Atmospheric Molecular Ions*

R. H. Neynaber, G. D. Magnuson, and S. M. Trujillo
Gulf Radiation Technology, A Division of Gulf Energy and Environmental Systems Company, San Diego, California 92112

and

B. F. Myers
Science Applications Incorporated, La Jolla, California 92037

(Received 10 August 1971)

Ion-molecule reactions between Ba and some atmospheric molecular ions have been studied using a merging-beams apparatus. The interaction energy W (i.e., relative kinetic energy in the center-of-mass system) was varied from 0.1 to 10 or 20 eV. The processes investigated were $Ba + O_2^+ \rightarrow BaO^+ + O$, $Ba + N_2^+ \rightarrow BaN^+ + N$, and $Ba + NO^+ \rightarrow BaN^+ + O$ and $Ba + NO^+ \rightarrow BaO^+ + N$. There is evidence that each process proceeds via a direct rather than a complex mechanism. In particular, in the center-of-mass system most of the product ions are scattered in the direction of the reactant Ba. Analysis of the kinetic energy of the products indicates that they are formed with considerable internal energy. The relative cross section for each of the reactions decreases as W increases. At $W = 0.1$ eV the absolute cross section for each process is of the order of 10^{-15} cm^2. Studies were made of the dependence of the cross section on internal excitation of the reactants.

I. INTRODUCTION

Experiments in which Ba is seeded in the upper atmosphere[1] have generated interest in the chemistry of Ba reacting with atmospheric constituents. In the present paper, merging-beam studies of ion-molecule reactions between Ba and some atmospheric molecular ions will be discussed. The interaction energy W (i.e., relative kinetic energy in the center-of-mass system) was varied from 0.1 to 10 or 20 eV. The processes investigated were

$$Ba + O_2^+ \rightarrow BaO^+ + O\ , \tag{1}$$

$$Ba + N_2^+ \rightarrow BaN^+ + N\ , \tag{2}$$

$$Ba + NO^+ \rightarrow \begin{cases} BaN^+ + O \\ BaO^+ + N\ . \end{cases} \tag{3}$$

The lab energy of Ba, of the ionic reactant, and of the ionic product will be denoted as E_1, E_2, and E_3, respectively.

II. APPARATUS

The above reactions were studied by measuring the product-ion current. For reaction (3), BaN^+ and BaO^+ were not resolved from each other. Only the total product-ion current was collected.

A schematic of the apparatus used in the experiments is shown in Fig. 1. The equipment was similar to that used for studying $H_2^+ + H_2 \rightarrow H_3^+ + H$ and described previously.[2] A retarding grid was not used, however, in the detector assembly. Instead, product ions were energy analyzed in an electrostatic hemispherical condenser. Resolution was improved by decelerating the ions before they entered the analyzer. Another modification was that the demerging magnet used in the $H_2^+ + H_2$ experiment was replaced with a demerging condenser. These modifications have been incorporated in another merging-beam apparatus, which has been successfully used for ion-molecule studies.[3]

Barium ions were generated in source 1 by surface ionization of Ba vapor at a hot tungsten filament. Figure 2 is a schematic of this source. The temperature, as read by the thermocouple, was approximately 600 °C. The potential of the W filament was 4050 V, which was equivalent to the desired energy of the reactant Ba. The potential of the anode was about 10 V less than the filament. A 10 V or greater potential difference between the filament and anode gave a minimum energy spread (i.e., full width at half-maximum) of approximately 1.5 eV for particles in a Ba^+ beam at 4050 eV. The spread was measured using a retarding-potential technique described previously.[4] Throughout this paper, a beam with such a spread is called monoenergetic. The energy of the beam, as determined by the same technique, agreed with the filament potential within a few eV. Therefore, beam energies are defined, for this paper, as equal to the filament potential. It is hypothesized that smaller potential differences between the filament and anode would allow the formation of a space charge between the filament and anode. Such a space charge could cause the energy spread to increase.

The barium ions were neutralized by charge transfer in a cell immediately following the analyzing magnet. The barium isotopes from the source were not resolved from each other in the magnet, and all of them entered the cell. The cell contained Na vapor. The ionization energies of Na and Ba

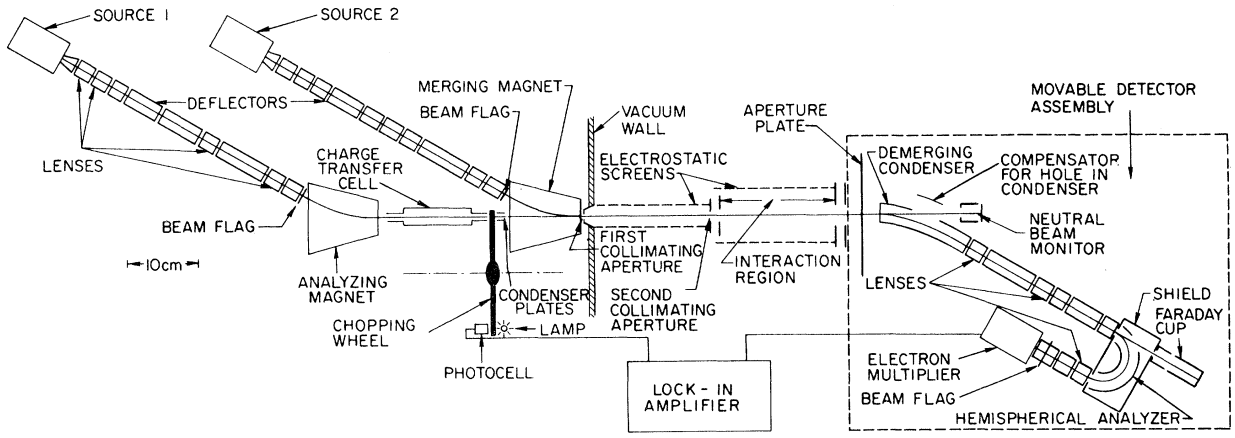

FIG. 1. Schematic of merging-beams apparatus. Apertures are not to the scale shown.

are 5.14 and 5.21 eV, respectively. The charge-transfer reaction was, therefore, nearly resonant. The resultant Ba neutral beam was mechanically chopped at 100 Hz.

The reactant molecular ions were generated in source 2. This was a magnetically confined oscillating-electron-bombardment source for N_2^+ and O_2^+. For reasons that are not understood, a sufficiently intense beam of NO^+ could not be obtained from this source. A nude ion gauge arrangement proved satisfactory for NO^+. Matheson gases were used. The minimum purities for N_2 (prepurified grade), NO (technical grade), and O_2 (extra dry grade) were 99.997, 98.5, and 99.6%, respectively.

A Bendix model M306-1 electron multiplier was employed as the detector for a few initial experiments. For most of the work, however, a Johnston model MM-1 electron multiplier was used. The latter had superior gain uniformity over its face. The output of the multiplier was fed into a lock-in amplifier.

III. KINEMATICS

Kinematics for reaction (2) are shown by the Newton diagram of Fig. 3. In this case the magnitude of the lab velocity of Ba, $|\vec{v}_{Ba}|$, is less than that of N_2^+, $|\vec{v}_{N_2^+}|$.

Since only an energy distribution of the product BaN^+ was measured, information was obtained on $|\vec{v}_{BaN^+}|$, but not on the directional properties of $\vec{v}_{BaN^+}$. Therefore, α and β (see Fig. 3) were not specifically determined. A comparison of the values of $|\vec{v}_{BaN^+}|$ with $|\vec{v}_c|$ can be used, however, to localize the angular scattering of BaN^+ in the center-of-mass sphere.

For reactions (1)–(3), β will be defined as the angle in the center-of-mass system between the velocity of Ba and of the product ion. Scattering in the center-of-mass system along the original Ba direction (i.e., $\beta = 0$) will be defined as forward scattering, whereas scattering opposite to the original Ba direction (i.e., $\beta = 180°$) will be defined as backscattering.

IV. METHOD

A. Absolute Cross Sections

Measurements for determining the absolute cross sections for reactions (1)–(3) were taken at $W = 0.1$ eV, where the signal-to-noise ratio was the best. The effects of transverse velocities are larger at smaller W (see Ref. 4). However, this drawback was not as serious as the increased difficulty (because of small signal-to-noise ratios) of obtaining sufficiently accurate absolute-cross-section data at higher W. The method for obtaining absolute cross sections has been described previously,[4,5] and, in general, applies to these experiments.

The lab-energy distribution of product ions was measured only for those ions generated inside the interaction region (see Fig. 1) by applying a potential P to this region. This potential was chosen to give the desired W. Outside of this region, the interaction energy was fixed at 30 eV by an appropri-

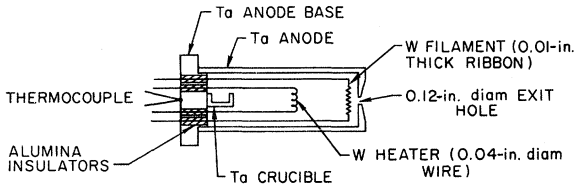

FIG. 2. Barium ion source. The anode is surrounded by three cylindrical stainless-steel heat shields (not shown). These are capped off at the end from which the ions emerge by two stainless-steel disks with appropriate apertures. The heater and filament are spot welded to 0.050-in. Ta rods which protrude through the alumina insulators into the anode. These rods are electrically connected to stand-off posts in a vacuum flange (not shown). The Ta crucible holds the barium charge.

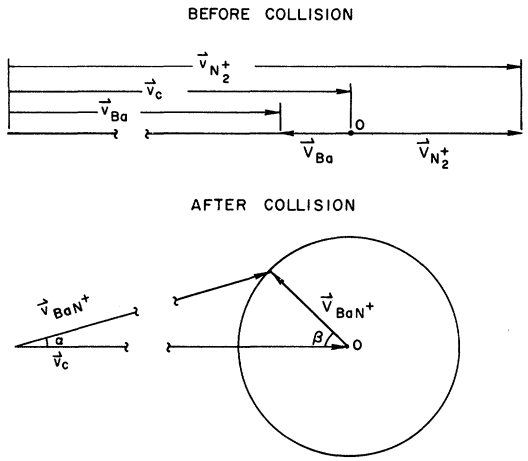

FIG. 3. Newton diagrams for $Ba + N_2^+ \rightarrow BaN^+ + N$. Subscript c refers to the c.m., $\vec{v}$ is for laboratory velocity, and $\vec{V}$ is for velocity in the c.m. system. The scattering angle in the lab system is α; in the c.m. system it is β. The drawing is not to scale.

ate choice of beam energies. At 30 eV the cross sections for reactions (1)–(3) are very small. The total product current generated inside the interaction region, which is the input signal to the multiplier, was obtained from the measured lab-energy distribution. This was accomplished by comparing the integral of this distribution with the integral of a distribution due to a monoenergetic beam of known intensity of Ba^+ from source 1. The energy of the monoenergetic beam was set equal to the energy at the peak of the measured distribution of product ions.

The multiplier response to the monoenergetic reference beam was slightly different from the response to the actual reaction products. This was because the particles impacting on the multiplier for the two cases had different masses and the product energies were actually a band of energies around the peak energy. Corrections to the total product current because of these factors are small and negligible compared to other experimental errors to be discussed.

It should be noted that for the measurements of product-energy distributions as well as the monoenergetic reference Ba^+ distribution, ions are swept over the same region of the multiplier face. Therefore, effects of nonuniform gain of the multiplier in this region do not appear in absolute-cross-section calculations.

The absolute value of the Ba current was obtained by measuring the secondary electron emission at the neutral-beam monitor due to that current. It was assumed that the secondary electron emission coefficient was equal to that for Ba^+ at the same energy. The coefficient for Ba^+ was measured immediately after the lab-energy distribution of product ions mentioned above was obtained.

The electron energy in source 2 was about 60 eV for absolute-cross-section measurements. An investigation of the effect of lower electron energies on measured cross sections will be discussed later.

B. Relative Cross Sections

Relative cross sections Q_R for reactions (1)–(3) were obtained over a range of W by measuring the lab-energy distributions of the product ions. The Q_R are proportional to the area under the distributions when these distributions are normalized to the same energy resolution of the detector assembly. For a given product-ion energy E_3, the resolution was obtained from the measured energy distribution of an essentially monoenergetic beam of Ba^+ at energy E_3 from source 1. The resolution was constant, within the error of the experiment, for all E_3 of interest associated with a given one of the above reactions.

The lab-energy distributions of product ions were measured for ions generated along the entire path of the merged beams rather than just in the interaction region. This was necessary to achieve the signal-to-noise ratios required for observations over the entire range of W that was studied. For the same reason, the electron energy in source 2 was kept at about 60 eV. The possibility of producing less excitation of the reactant molecular ions at lower electron energy had to be forfeited.

For reactant beams outside of the interaction region, larger transverse velocities can exist than for those inside. These transverse velocities can affect W and relative-cross-section measurements, particularly at low W.[4] To investigate this, relative cross sections for reaction (2) were obtained at $W = 0.1$, 1, and 5 eV for ions generated along the entire path of the merged beams and for ions generated only in the interaction region. Within experimental error, the cross sections were the same for the two cases. This indicates that additional complications due to transverse velocities were not introduced in these relative-cross-section measurements by collecting ions outside as well as inside the interaction region.

Several tests were made to assure the validity of the relative-cross-section measurements. One of these was to check for the loss of any product ions caused by angular scattering following the reaction. This test was made by inserting a smaller aperture in front of the demerging condenser than was normally used, and looking for a loss in signal. This test was made for low and high W. No change of signal was ever observed.

Another test was to check the absolute transmission of the detector assembly for ions over the lab-energy range of product ions from reactions

(1)–(3). The test was normally made by using a beam of Ba^+ from source 1. The transmission is defined as the current measured at the beam flag in front of the electron multiplier divided by the current at the neutral-beam monitor. For these measurements the flag, together with the electrode upstream from it, were used as a Faraday cup. The transmission for all experiments was 100% within experimental error.

Checks for linearity of product-ion currents with primary-beam currents were also made. Such linearity was affirmed before proceeding with the experiments. Another important test was to establish the independence of cross sections upon E_1 and E_2 for the same W. This could be shown even when E_1 and E_2 were changed so that the relative velocities of Ba and of the reactant molecular ions of interest were reversed in direction.

C. Dependence of Cross Section on Electron Energy

In order to investigate the effect of excitation of the reactant molecular ions on the measured cross sections, the electron energy in source 2 was decreased below 60 eV. This was done for reactions (1)–(3) only at $W = 0.1$ eV and for product ions generated along the entire path of the merged beams.

The reactant-molecular-ion current diminished markedly when the electron energy was lowered. The resultant small signal-to-noise ratios prevented the measurement of entire energy distributions of the product ions. Consequently, the product-ion current was measured only at an energy equal to that of the peak of the distribution obtained when the electron energy was 60 eV.

These measured currents at the low electron energy were compared with the peak currents for 60-eV electrons in order to assess the effects of excitation of the reactant molecular ions. The ratio of currents (normalized to the same primary-beam currents and gain setting of the lock-in amplifier system) for low-energy electrons and 60-eV electrons will be called R. The results will be discussed later.

The electrons in source 2 had a distribution of energies. The maximum energy of a given distribution was equal to the dc potential difference between the anode and the filament plus one-half the peak voltage across the secondary winding of the center-tapped ac filament transformer. When the source was operated in the low-energy electron mode, the maximum electron energy for reactions (1), (2), and (3) was $15.0 + 2.4 = 17.4$, $17 + 2.2 = 19.2$, and $12.2 + 3.3 = 15.5$ eV, respectively. The first and second figures in these sums are the above mentioned dc and ac potentials, respectively. Most of the electrons had energies less than the maximum energy. For the low electron energies the gas pressure in the ion source was carefully monitored to be sure that it was sufficiently low that the mean free path of electrons for ionization was long compared to the length of the region of ionization. It is conceivable that the residence time of ions in the source was sufficiently long that a small percentage of these ions could collide more than once with an electron. Such events would allow these ions to have excess internal energy. An extraction field was used to minimize this potential problem.

D. Cross Sections for Ground-State and Metastable Ba

Although there was no excited Ba^+ leaving source 1, there could have been some metastable $Ba(^3D)$ coming from the charge-transfer cell. This is the lowest-lying metastable state of Ba and is 1.12 eV above the ground state $Ba(^1S)$.

The energy defects for charge transfer to the ^1S state and to the ^3D state are $+0.07$ and -1.05 eV, respectively. Theoretical asymmetric-charge-transfer curves obtained by Rapp and Francis[6] can be used to give a rough estimate of the cross-section ratio for these two cases. At the lab energy of Ba^+ in these experiments, it is determined from these curves that the cross section for charge transfer to the ^1S state is of the order of 50 times that for charge transfer to the ^3D state. Thus, only a few percent of the Ba particles could be expected to be in the ^3D state.

There was the possibility that the cross sections for reactions (1)–(3) are considerably larger for $Ba(^3D)$ than for $Ba(^1S)$. If this were the case, a small percentage of $Ba(^3D)$ could have a disproportionately large effect.

This possibility was investigated by using K in the charge-transfer cell instead of Na. The energy defects for charge transfer of Ba^+ to $Ba(^1S)$ and to $Ba(^3D)$ are $+0.87$ and -0.25 eV, respectively. The cross section for charge transfer to the ^3D state is considerably larger than that for charge transfer to the ^1S state and could be as much as 10 to 15 times larger.[6] Thus, with K in the cell, most of the Ba particles were in the metastable state. With Na in the cell, most were in the ground state. At $W = 0.1$ eV the peak heights of the energy distributions of ions generated along the entire path of the merged beams were measured and compared for these two cases. The results that were obtained and their interpretation will be discussed later in Secs. V and VI.

The cross section for quenching $Ba(^3D)$ to $Ba(^1S)$ in potassium vapor is unknown. At the pressure of potassium vapor that existed in this experiment a value of about 10^{-14} cm^2 would have been necessary to reduce the beam intensity to $1/e$ times the nonquenched value. We assume that the cross section is considerably smaller than 10^{-14} cm^2, and

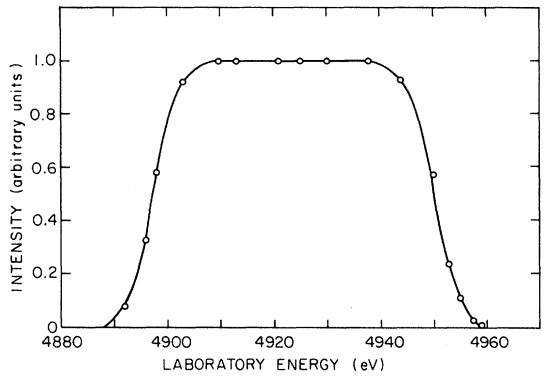

FIG. 4. Lab-energy distribution of a monoenergetic beam of Ba^+ measured with detector assembly. This distribution was measured with the electrostatic hemispherical analyzer and with 100% transmission. The actual energy and an upper limit to the energy spread of the Ba^+ beam, as determined by a retarding potential technique, was 4913 and 1.5 eV, respectively.

therefore that quenching in this experiment is negligible.

V. RESULTS

The lab-energy distribution of a monoenergetic beam of Ba^+ from source 1 at an energy of 4913 eV is shown in Fig. 4. The energies in the distribution were determined from settings of the electrostatic hemispherical analyzer. It is noted that the energy spread of this distribution, or the resolution of our detector assembly, is about 1% of the nominal energy. For this resolution the transmission of the assembly is 100%. The resolution can be improved by further decelerating the ions before they enter the hemispherical analyzer. This can be done only at the expense of the transmission. For the experiments described in this paper the resolution was kept constant, and the transmission was always 100%.

The center of symmetry of the distribution in Fig. 4 is about 4923 eV. This indicates that energies, as determined by the hemispherical analyzer, have a systematic error of about −0.2%. Corrections to such energies were not made.

The measured lab-energy distributions of ionic products from reaction (1)–(3) are shown in Figs. 5–7. The distributions have been normalized so that their peak intensities are equal. For most of the curves the data points were taken only once. For a few curves they were taken more than once and were reproducible. Ratios of peak heights for the distributions were checked periodically over a period of months and were also reproducible.

As W increased, the signal-to-noise ratios for the distributions decreased. Above the maximum W shown in Fig. 5–7, the signal-to-noise ratio was too small for obtaining reasonably accurate distributions.

The resolution of the detector assembly was not sufficiently good to separate the two ionic products of reaction (3). Therefore, the distributions shown in Fig. 7 are composites for BaN^+ and BaO^+.

The lab energies associated with the arrows in Figs. 5–7 were calculated assuming that each ionic

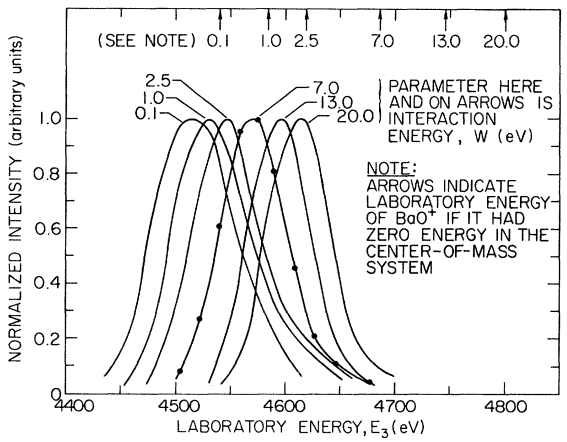

FIG. 5. Lab-energy distributions of BaO^+ from $Ba + O_2^+ \rightarrow BaO^+ + O$ (Ba slower than O_2^+ and $E_1 = 4050$ eV). The distributions have been normalized so that their peak intensities are equal. Each arrow denotes the calculated lab energy of BaO^+ for a given W (indicated in electron volts by the associated number) assuming that BaO^+ has a lab velocity equal to that of the center of mass. Some distributions and all data points except those for one curve have been omitted for clarity.

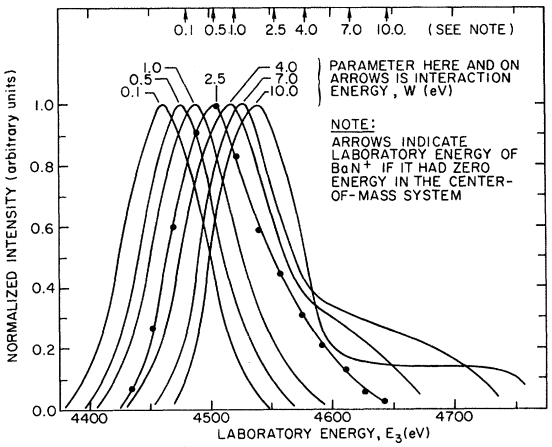

FIG. 6. Lab-energy distributions of BaN^+ from $Ba + N_2^+ \rightarrow BaN^+ + N$ (Ba slower than N_2^+ and $E_1 = 4050$ eV). The distributions have been normalized so that their peak intensities are equal. Each arrow denotes the calculated lab energy of BaN^+ for a given W (indicated in eV by the associated number) assuming that BaN^+ has a lab velocity equal to that of the center of mass. Some distributions and all data points except those for one curve have been omitted for clarity.

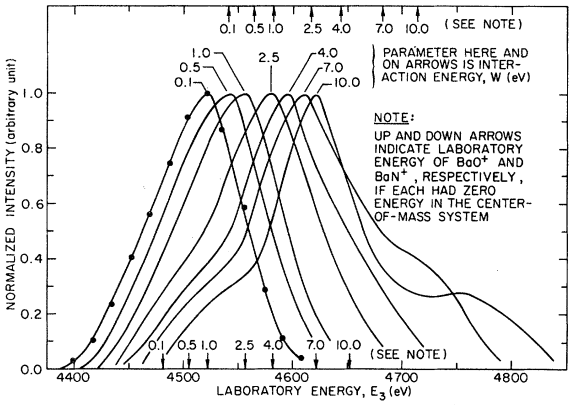

FIG. 7. Lab-energy distributions of BaN^+ and BaO^+ from $Ba + NO^+ \rightarrow \begin{matrix} BaN^+ + O \\ BaO^+ + N \end{matrix}$ (Ba slower than NO^+ and $E_1 = 4050$ eV). The distributions have been normalized so that their peak intensities are equal. The arrows pointing up and down denote the calculated lab energies of BaO^+ and BaN^+, respectively, assuming that each has a lab velocity equal to that of the center of mass. The numbers associated with the arrows indicate W in eV for each calculated lab energy. Some distributions and all data points except those for one curve have been omitted for clarity.

product has a lab velocity equal to that of the center of mass. The W for each calculation is indicated next to the arrow.

Figure 8 shows relative cross sections as a function of W for reactions (1)–(3). These were obtained from energy distributions as described previously. The cross sections have been normalized to unity at $W = 0.1$ eV for each process. The error brackets indicate increased uncertainty as W increases.

Values of the absolute cross section at $W = 0.1$ eV for reactions (1)–(3) are given in Table I. For each reaction, two cross sections are given: Q_H for 60-eV electrons in the ion source and Q_L for considerably lower-energy electrons. The method for obtaining Q_H has been discussed. The Q_L are obtained by multiplying the Q_H by R. Implicit in this procedure is the assumption that the energy distributions of product ions for 60-eV and low-energy electrons are the same. This facet will be discussed at greater length later.

TABLE I. Absolute cross sections at $W = 0.1$ eV for 60-eV and low-energy electrons.

Reaction	Q_H[a] (10^{-15} cm^2)	Low-energy[b] (eV)	R[c]	Q_L[d] (10^{-15} cm^2)	Error in Q_L (%)
(1)	0.9	17.4	3.0	2.7	+47 −40
(2)	2.4	19.2	1.17	2.8	+44 −31
(3)	1.2	15.5	0.75	0.9	+47 −40

[a]Cross section for 60-eV electrons.
[b]Maximum energy in low-energy electron distribution.
[c]Defined previously.
[d]Cross section for low-energy electrons.

The estimated error in Q_L of Table I is a composite of systematic and random errors. The systematic error for reactions (1) and (3) consists of the following: −5 to +10% error in the secondary electron emission coefficient of Ba at the neutral-beam monitor, +15% for transverse-velocity effects, +25% in the overlap integral, and −25% to +17% in R. The random error is assumed to be ±30%. The estimated errors for reaction (2) are the same as those above except for R, whose error is estimated as −5% to +10%.

As mentioned previously, at $W = 0.1$ eV the peak heights of the energy distributions of ions generated along the entire path of the merged beams were measured first with Na in the charge-transfer cell and then with K. The ratio of peak heights will be called r. For reactions (1), (2), and (3), r equals 1.85, 0.79, and 0.67, respectively. No corrections to absolute cross sections were made for the existence of Ba in the ^3D state. The reason for making

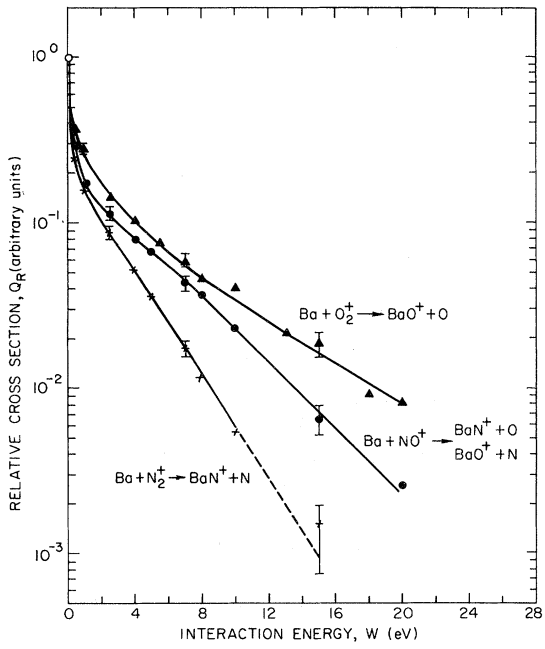

FIG. 8. Relative cross sections for some ion-molecule reactions involving barium. The cross sections for each of the processes have been normalized to unity at $W = 0.1$ eV. The curves are drawn by eye to give the best fit to the points. The electron energy in the molecular-ion source was approximately 60 eV for all the measurements. Some typical error brackets are shown. The relative cross section at $W = 15$ eV is sufficiently uncertain for $Ba + N_2^+$ that an extrapolation (dashed portion of curve) is made to this energy.

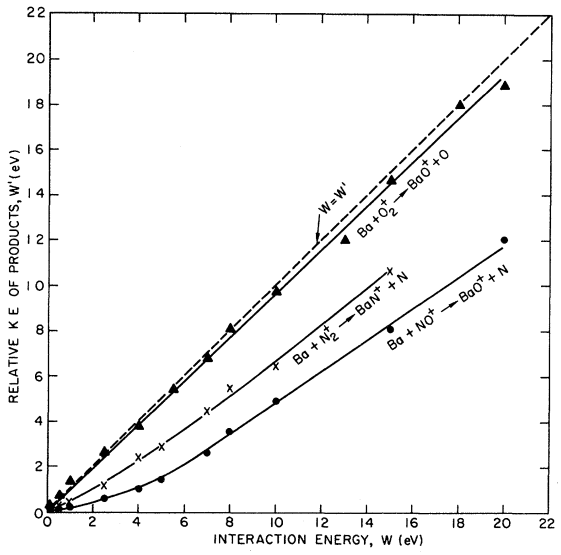

FIG. 9. Relative kinetic energy (KE) of products vs W for some ion-molecule reactions involving barium. The points shown were calculated for the case where the lab energy of the product molecular ion was equivalent to that at the peak of the measured energy distribution and under the assumption that $\beta = 0$. For the reaction $Ba + NO^+$, it was assumed that only the product-ion BaO^+ contributed to the peak of the energy distribution. The curves are drawn by eye (through the origin) to give the best fit to the points.

no corrections will be given in Sec. VI.

Figure 9 shows W', the relative kinetic energy of the products in the center-of-mass system, as a function of W. The W' were calculated for lab energies of the product ions corresponding to those of the peaks of the measured energy distributions. It was assumed that the product ions were scattered in the forward direction, i.e., $\beta = 0$.

VI. DISCUSSION OF RESULTS

From Fig. 5 it is noted that each energy distribution is fairly symmetric about the energy at the peak. This will be of interest when comparisons are made with the energy distributions of reactions (2) and (3).

The energy of the peak of each distribution in Fig. 5 is less than that of the associated arrow. This indicates that most of the BaO^+ in a given distribution is confined to scattering angles β in the center-of-mass system of less than 90°. It is noted that the percentage of BaO^+ at angles less than 90° increases as W increases. In fact, for $W > 2.5$ eV virtually all of the BaO^+ is scattered at angles less than 90°. This suggests that reaction (1) becomes more directed for increasing W.

As mentioned previously, β's were not specifically determined. It is conceivable, in fact not unlikely, that the β's for each distribution are confined either to a small range of angles near 0°, or to two small ranges—one near 0° and the other near 180°. A sticky collision complex would result in a nondirected reaction, but of the many hundreds of ion-molecule reactions studied only a few such complexes have been found.[7] For most of the studied reactions the energy distributions of the products peak in the forward or backward direction.

Below $W = 2.5$ eV the distributions in Fig. 6, like those in Fig. 5, are nearly symmetric about the peak energy. At 2.5 eV and above, each curve has a high-energy tail which at the higher W's looks like a low-intensity unresolved peak. From the relationship of the arrows and the lab energies of the tails, it can be said that for the greater portion of the BaN^+ associated with these tails, $\beta > 90°$. For most of the BaN^+ not associated with the tails (i.e., that associated with the major peak), $\beta < 90°$, just as it is in Fig. 5. Therefore, in the center-of-mass system the direction of BaN^+ associated with the secondary peak is in a direction generally opposite to that of the reactant Ba (i.e., backscattering), whereas the direction of BaN^+ associated with the major peak is in a direction generally the same as that of Ba (i.e., forward scattering). This could be the case if the impact parameter were considerably smaller for products ending up in the secondary rather than the major distribution.

It would be reasonable to assume that the secondary distribution is caused by BaN^+ from an endothermic process occurring for $W \geq 2.5$ eV. Such a process should become more favorable for a small impact parameter. If all of the impact parameters associated with the secondary process were small, the corresponding cross section would be small. It follows (as observed) that the backscattering process would be dominated by the forward-scattering process. A related analysis of major and minor peaks appearing in the data from another experiment has been made previously.[8]

The energy distributions for reaction (2), then, appear to consist of two components. One of these is due to BaN^+ scattered mainly in the forward direction, and the other is due to BaN^+ scattered mainly in the backward direction. The energy distributions for reaction (1) consist of only one component, which is due to BaO^+ scattered primarily in the forward direction.

The energy distributions of product ions for reaction (3) are shown in Fig. 7. These distributions seem to consist of three components. For $W < 2.5$ eV, the asymmetry of the distribution about the peak energy suggests the existence of more than one component. This asymmetry is caused by a low-energy tail. It seems likely that this tail is due to forward-scattered BaN^+, whereas the major part of the distribution is caused by forward-scattered BaO^+. For $W > 2.5$ eV the low-energy tail

begins to look like an unresolved peak. The lab energy of each unresolved peak and its associated primary peak appear to differ by a percent or so. This is expected if the above interpretation is correct, since the percentage difference in the lab energy between similarly directed BaN^+ and BaO^+ in a merging-beams experiment would be the percentage difference between the masses–viz, about a percent. This follows from the fact that the basic concept of merging beams requires that all reactants and products in a given reaction have nearly the same lab velocity.

By comparing the energies in the BaO^+ and BaN^+ distributions of Fig. 7 with the associated arrows, it is clear that $\beta < 90°$ for most of the particles in the distributions. As W increases, a larger fraction of the particles in the distributions are forward scattered; i.e., the reaction becomes more directed. This is the same conclusion reached for reaction (1) and for the main component of the distributions for reaction (2).

Finally, in Fig. 7 we note a high-energy tail for $W \geq 4$ eV, which might indicate a third component in the distribution. Some evidence of such a component may be seen from Fig. 7 at even lower W. This could very likely be due to backscattered BaO^+ and/or BaN^+. Supporting arguments for this interpretation would be similar to those for the secondary distributions of Fig. 6.

In Fig. 8 the relative-cross-section curve for reaction (3) has a definite inflection near $W = 4$ eV. As noted above, the energy distributions for this reaction indicate a new process occurring at or near this same W. It is suggested that the inflection in the relative curve is another indication of this new process. The relative-cross-section curve of a reaction studied in another experiment,[8] which was mentioned previously, actually exhibits a maximum instead of an inflection. The maximum occurred in the energy region where the opening up of an endothermic process was hypothesized.

From the energy distributions for reaction (2) it was proposed that a new process became accessible at $W = 2.5$ eV. Since a new process for reaction (3) appears to induce an inflection in the relative-cross-section curve at the W for its onset, an inflection might occur in the relative-cross-section curve for reaction (2) at or near $W = 2.5$ eV. There is no definite indication of an inflection here in Fig. 8. However, it does not appear unlikely that such an inflection exists, but is washed out in the scatter of the data.

The energy distributions for reaction (1) suggests the existence of only one process. On the basis of our observations concerning reactions (2) and (3), it would be reasonable to expect no inflections in the relative-cross-section curve for reaction (1). It seems fair to say that, from Fig. 8, the relative-cross-section curve for reaction (1) appears the least likely of all the reactions to have an inflection.

Figure 9 will be used to conjecture about the disposition of the reactant energy in the center-of-mass system (i.e., relative kinetic energy and internal energy) for reactions (1)–(3). It can be shown from measured values of the ionization potential of BaO (i.e., 6.5 eV)[9] and of the bond energy of BaO (i.e., 5.8 eV)[10] that reaction (1) is exothermic by about 6.3 eV for ground-state reactants and products. Since W' is almost equal to W, the exothermicity must be absorbed in internal energy of the products. If the reactants in our experiment were excited, then the internal energy of the products would be increased by the amount of this excitation.

The ground state of BaO^+ will dissociate into $Ba^+ + O$ when 4.5 eV is absorbed in the bond. Therefore, if the products of reaction (1) do absorb 6.3 eV, BaO^+ may be electronically excited.

The near equality of W' and W depends, of course, upon the assumptions made in calculating the W' of Fig. 9. If $\beta \neq 0$, then W' will be larger than the values shown in the figure, and the internal energy absorbed by the products will be less than that mentioned above. Calculations for $\beta \neq 0$ have been made under the assumption that the products have zero internal energy (ground-state reactants were also assumed for the calculations) together with the assumption that the lab energy of the product molecular ions is equal to that at the peak of the measured energy distribution. The first assumption infers that the exothermicity of 6.3 eV as well as W is all converted into W'. These β's range from about 60° at $W = 0.1$ eV to 30° at $W = 20$ eV. The corresponding α's are a few degrees and would not reduce the collection efficiency of the product ions.

It is not suggested that the energy distributions of BaO^+ will peak at the β's mentioned above. The calculations were only made to show that, in principle, all of the exothermicity of reaction (1) could go into W', a quite different result from that concluded from Fig. 9. Another possibility is that the peak of a distribution has a range of β's associated with it and, hence, a range of internal energies associated with the products. Similar conclusions about the relative kinetic energy and internal energy of the products can be reached for points other than the peaks of the distributions.

The curve in Fig. 9 labeled $Ba + NO^+ \rightarrow BaO^+ + N$ was obtained under the assumption that not only does $\beta = 0$ but also that only the product-ion BaO^+ of reaction (3) contributes to the peak of the energy distribution. From our previous discussions it appears that, in the region of the energy distribution near the peak, BaO^+ is the dominant ion.

The exothermicity of $Ba + NO^+ \rightarrow BaO^+ + N$ is about 2 eV for ground-state reactants and products. If β does indeed equal zero, then from Fig. 9 the internal energy of the products must be $(W - W') + 2$ eV. At $W = 20$ eV, for example, $W - W' = 8.3$ eV. Therefore, 10.3 eV must go into internal energy of the products.

The bond energy and ionization potential of BaN are not known. Since the relative-cross-section curve of reaction (2) is qualitatively like those of reactions (1) and (3), it appears as if reaction (2) is exothermic. Furthermore, because the W' vs W curve for this reaction falls in between those of (1) and (3), the general conclusions reached for the latter reactions concerning the disposition of reactant energy and exothermicity also apply to reaction (2).

Table I gives absolute cross sections at $W = 0.1$ eV for reactions (1)–(3) for low- and high-energy electrons in the molecular-ion source. The ratio Q_L/Q_H should be proportional to the ratio of the areas of the lab-energy distribution curves of the product ions for low- and high-energy electrons, respectively, when these curves are normalized to the same primary-beam currents and gain setting of the lock-in amplifier system.

The Q_L of Table I are obtained by multiplying the Q_H by R. This procedure would be correct if the two normalized energy distributions were identical. It is conceivable that the energy distribution of the product ions for high electron energy is wider than that for low electron energy because of the possibility for more product channels at the higher electron energy and/or the conversion of internal energy of the reactants into translational energy of the products. The presence of product channels, in addition to those that have been identified, does not appear to exist from a further analysis of Figs. 5–7. The presence of the identified channels probably does not require internal excitation of the reactant molecular ions. The conversion of internal energy of the reactants into translational energy of the products would be more probable if an intermediate complex were formed. Evidence indicates, however, that the reactions are direct. Therefore, a wider energy distribution of product ions at the high electron energy seems unlikely. If, however, such an effect exists, the quoted Q_L would be too large.

Another possibility is that the peaks of the energy distributions for low and high electron energy are not at the same lab energy for the same reasons that the widths of the distributions would not be the same. Again, this possibility seems remote. If the lab energies of the peaks are different, however, the quoted R and Q_L will be too small. This effect, then, would tend to nullify that due to different widths of the distributions.

For reaction (1) the maximum electron energy in the low-energy electron distribution was 17.4 eV. The only electronic states of O_2^+ that could exist in the interaction region at this energy would be the ground state and the metastable $^4\Pi_u$ state whose threshold is at about 16.1 eV.[11] Since most of the electrons have energy less than 17.4 eV and this energy is not much greater than the threshold for the production of O_2^+ in the $^4\Pi_u$ state, very little of the O_2^+ will be in the metastable state. The results of Turner *et al.*,[12] who used a similar O_2^+ source in their experiments, verify this conclusion.

At 60-eV electron energy it is assumed that only the ground and $^4\Pi_u$ state are present in the interaction region and that about 30% of the O_2^+ is in the $^4\Pi_u$ state. This is based on the work of Turner *et al.*[12]

If it is assumed that the cross section for reaction (1) is zero for the $^4\Pi_u$ state of O_2^+ and that no O_2^+ is in the $^4\Pi_u$ state at the low electron energy, then Q_L (as obtained by correcting Q_H from Table I) would have been about 1.3×10^{-15} cm^2. Since Q_L was actually 2.7×10^{-15} cm^2, it is assumed that O_2^+ in metastable vibrational levels of the ground electronic state plays a role in this study. Since such levels would be more highly populated at the higher electron energy [where the cross section for reaction (1) is smaller], it is assumed that vibrationally excited states of O_2^+ tend to reduce the cross section for reaction (1).

For reaction (2) the maximum electron energy in the low-energy-electron distribution was 19.2 eV. The lifetimes of the electronic states of N_2^+ are such that only N_2^+ in the ground and first electronic states will merge with Ba. It is conceivable that the population of the states of N_2^+ was about the same for low- and high-energy electrons since the difference between Q_L and Q_H is only 17%.

For reaction (3) the maximum electron energy in the low-energy electron distribution was 15.5 eV. At this energy there can be no electronically excited states of NO^+.[13] If the Franck-Condon rules apply for electron impact ionization of NO, about 93% of the NO^+ will be in the $v = 0$ through $v = 3$ vibrational levels and 7% in the $v = 4$ through $v = 8$ levels.[14]

Since $Q_H > Q_L$, it appears as if internal excitation of NO^+ (induced by 60-eV electrons) enhances the rate of reaction (3). This is the opposite effect for internal excitation of the reactant molecular ions of reactions (1) and (2).

In some recent experiments, Clendenning *et al.*[15] have collided a beam of Ba with a magnetically confined afterglow of a Lyman-α photoionized plasma containing NO^+. It is concluded from these experiments that the thermal-energy cross section for reaction (3) is $\leq 4 \times 10^{-16}$ cm^2. The products BaN^+ and BaO^+ were not resolved from each other.

All of the NO^+ was in the $v=0$ through $v=3$ vibrational levels of the ground electronic state.

An extrapolation of the present cross-section measurements for reaction (3) to thermal energy by extending the observed monotonic behavior at higher energies indicates a cross section greater than 2×10^{-15} cm^2. If this extrapolation is valid, it is conceivable that the resultant discrepancy between the two results can be explained by invoking a large enhancement of the cross section for $v>3$.

Another explanation would be that the cross section for reaction (3) at $W=0.1$ eV is about 10^{-15} cm^2 as obtained in the present work and has the value of Clendenning *et al.* at thermal energy. It would appear that an activation energy would have to be hypothesized for this explanation since $Ba+NO^+ \rightarrow BaO^+ + N$ is known to be exothermic and has been shown to be the dominant process in reaction (3).

As mentioned previously, only a few percent of Ba was in the metastable ^3D state when Na was in the charge-transfer cell. This, together with the fact that r was within a factor of 2 from unity, implied that no corrections to absolute cross sections were necessary for the existence of Ba in the ^3D state.

The ratio of the peak heights of the lab-energy distributions of the product ions for Na and K in the charge-transfer cell is assumed to be equal to the ratio of the areas of these distributions. The reasons for this assumption are analogous to those presented in the analysis of the cross-section dependence on the energy of the electrons in the reactant-ion source.

The measured relative cross sections for reactions (1)–(3) do not fit the Langevin model[16] which predicts a $W^{-1/2}$ dependence. They also do not fit a spectator stripping model.[17] This model predicts a specific lab energy for each W rather than a distribution of energies and a linear relationship between W' and W. The slope of the experimental straight line for W' vs W for reaction (1) shown in Fig. 9 is about a factor of 2 larger than that predicted by the spectator stripping model.

ACKNOWLEDGMENTS

The authors wish to thank Dr. P. K. Rol and Dr. D. A. Vroom for many valuable suggestions and helpful discussions during these experiments.

---

*Supported by the Advanced Research Projects Agency through the Office of Naval Research under Contract No. N00014-70-C-0037.

[1]G. Haerendel and R. Lüst, Sci. Am. 219, 81 (1968).

[2]R. H. Neynaber and S. M. Trujillo, Phys. Rev. 167, 63 (1968).

[3]P. K. Rol and E. A. Entemann, J. Chem. Phys. 49, 1430 (1968).

[4]S. M. Trujillo, R. H. Neynaber, and E. W. Rothe, Rev. Sci. Instr. 37, 1655 (1966).

[5]R. H. Neynaber, S. M. Trujillo, and E. W. Rothe, Phys. Rev. 157, 101 (1967).

[6]D. Rapp and W. E. Francis, J. Chem. Phys. 37, 2631 (1962).

[7]A. Henglein, in *Proceedings of the International School of Physics, Enrico Fermi Course* XLIV, edited by Ch. Schlier (Academic, New York, 1970), p. 147.

[8]K. L. Wendell and P. K. Rol, *Abstracts of the Seventh International Conference on the Physics of Electronic and Atomic Collisions* (North-Holland, Amsterdam, 1971), p. 989.

[9]G. Mesnard, R. Uzan, and B. Caband, Cahiers Phys. 17, 333 (1963).

[10]B. Darwent, Natl. Std. Ref. Data Ser., Natl. Bur. Std. (U.S.) NSRDS-NBS 31, 15 (1970).

[11]F. Gilmore, J. Quant. Spectry. Radiative Transfer 5, 369 (1965).

[12]B. R. Turner, J. A. Rutherford, and D. M. J. Compton, J. Chem. Phys. 48, 1602 (1968).

[13]K. P. Huber, Can. J. Phys. 46, 1691 (1968).

[14]M. Halmann and I. Laulicht, J. Chem. Phys. 43, 1503 (1965).

[15]L. M. Clendenning, S. Studniarz, and W. L. Fite, University of Pittsburgh (private communication).

[16]P. Langevin, Ann. Chim. Phys. 5, 245 (1905).

[17]A. Henglein, in Ref. 7, p. 154.